Electronic Supplementary Material (ESI) for ChemComm.

Cyano Modified Triphenylmethyl Radical Skeletons: Higher Stability and Efficiency

Kuo Lv†, Minzhe Zhang†, Xin Xia, WenJing Liu, Keke Wan, Ming Zhang and Feng Li*

State Key Laboratory of Supramolecular Structure and Materials, College of Chemistry, Jilin University Changchun, 130012, P. R. China

*E-mail: lifeng01@jlu.edu.cn

Contents

General information

All reagents and solvents required for synthesis and characterization are purchased from commercial suppliers and used directly without any treatment. The nuclear magnetic resonance (^{1}H NMR) spectra were recorded on the Bruker AVANCEIII 500 spectrometer at 500 MHz at 298 K and tetramethyl silane (TMS) (δH = 0 ppm) as the internal standard. MALDI-TOF mass spectra were recorded on a Brucker Autoflex speed TOF/TOF mass spectrometer with DCTB as a matrix. UV–vis absorption spectra were recorded on the model UV-vis-2550 spectrophotometer. Fluorescence spectra were carried out using the model RF-6000 Spectro-fluorophotometer. The electrochemical oxidation and reduction potentials were recorded using an electrochemical analyzer (CHI660C, CH Instruments, USA). The femtosecond transient absorption spectrometer Helios Fire (Ultrafast Systems LLC, USA) was used to test the ultrafast absorption spectrum with a delay resolution of 14 fs. The fluorescence decay spectra and PLQY were recorded on an Edinburgh fluorescence spectrometer (FLS980), and the lifetime of the excited states was measured by the time-correlated single photon counting method under the excitation of a laser (378 nm). Elemental analysis (C, H and N) was performed on a Elementar Vario micro cube elemental analyzer. Thermal gravimetric analysis (TGA) was characterized by a TAINSTRUMENTS Q500 TGA analyzer. DFT and TD-DFT calculations were performed on Gaussian09 series of programs using the UB3LYP function and 6-31G(d,p) basis.[1]

1. Synthesis Section

HTTM was prepared as reported.[2]

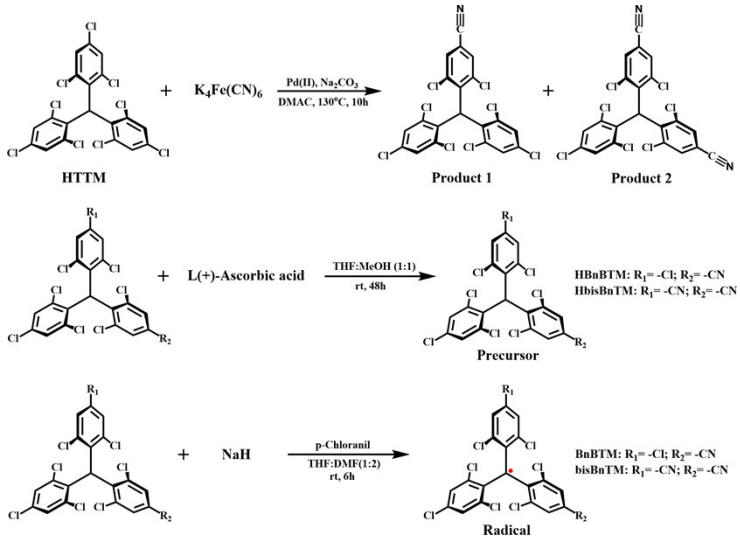

Scheme S1. The synthesis route of BnBTM and bisBnTM.

(1) Synthesis of Product 1 and Product 2.[3]

Dichlorobis[di-*tert*-butyl(*p*-dimethylaminophenyl)phosphino]palladium(II) (0.14 g, 0.2 mmol), HTTM (1.11 g, 2.0 mmol), potassium hexacyanoferrate(II) (1.69 g, 4.6 mmol), and sodium carbonate (0.49 g, 4.6 mmol) were dissolved in dry *N*,*N*-dimethylacetamide (20.0 mL) under a nitrogen atmosphere. The reaction mixture was stirred at 130 °C for 10 h. After cooling to room temperature, the solution was extracted with dichloromethane. Organic layer washed five times with water and dried. The solvent was removed under vacuum and the crude product was purified by silica gel column chromatography (using petroleum ether: dichloromethane = 5:1 v/v). Products 1 (0.27 g, 25% yield) and 2 (0.27 g, 25% yield) were obtained as pink and red solids, respectively.

(2) Preparation of HBnBTM and HbisBnTM

Products 1 (0.54g, 1.0mmol) was dissolved in a mixture of tetrahydrofuran (30.0 ml)

and methanol (30.0 ml) solutions. Then, L (+)-Ascorbic acid (3.52g, 20.0mmol) was added at ambient conditions. After stirring at room temperature for 48 h, the solution was extracted with dichloromethane. The obtained organic layer was collected and dried and the solvent was removed under vacuum. Crude product was purified by silica gel column chromatography (using petroleum ether: dichloromethane = 8:1 v/v). HBnBTM was obtained as a white solid (0.49 g, 90% yield). ^{1}H NMR (500 MHz, CD2Cl2) δ 7.65 (d, J = 1.7 Hz, 1H), 7.53 (d, J = 1.7 Hz, 1H), 7.41 (dd, J = 6.4, 2.2 Hz, 2H), 7.28 (dd, J = 8.4, 2.2 Hz, 2H), 6.75 (s, 1H). MALDI-TOF-MS (m/z): calculated for $C_{20}H_7Cl_8N$, 544.8028; found, 543.6005. Elem. Anal. Calcd for $C_{20}H_7Cl_8N$: C 44.09, H 1.29, N 2.57; found, C 43.69, H 1.43, N 2.58.

HbisBnTM was obtained by the same method.

Products 2 (0.53g, 1.0mmol) was dissolved in a mixture of tetrahydrofuran (30.0 ml) and methanol (30.0 ml) solutions. Then, L (+)-Ascorbic acid (3.52g, 20.0mmol) was added at ambient conditions. After stirring at room temperature for 48 h, the solution was extracted with dichloromethane. The obtained organic layer was collected and dried and the solvent was removed under vacuum. Crude product was purified by silica gel column chromatography (using petroleum ether: dichloromethane = 4:1 v/v).

HbisBnTM was obtained as a white solid (0.49 g, 92% yield). ^{1}H NMR (500 MHz, CD2Cl2) δ 7.67 (dd, J = 6.1, 1.7 Hz, 2H), 7.54 (dd, J = 8.0, 1.7 Hz, 2H), 7.43 (d, J = 2.2 Hz, 1H), 7.30 (d, J = 2.2 Hz, 1H), 6.81 (s, 1H). MALDI-TOF-MS (m/z): calculated for $C_{21}H_7Cl_7N_2$, 533.8399; found, 533.3288. Elem. Anal. Calcd for $C_{21}H_7Cl_7N_2$: C 47.11, H 1.32, N 5.23; found, C 47.85, H 1.67, N 5.23.

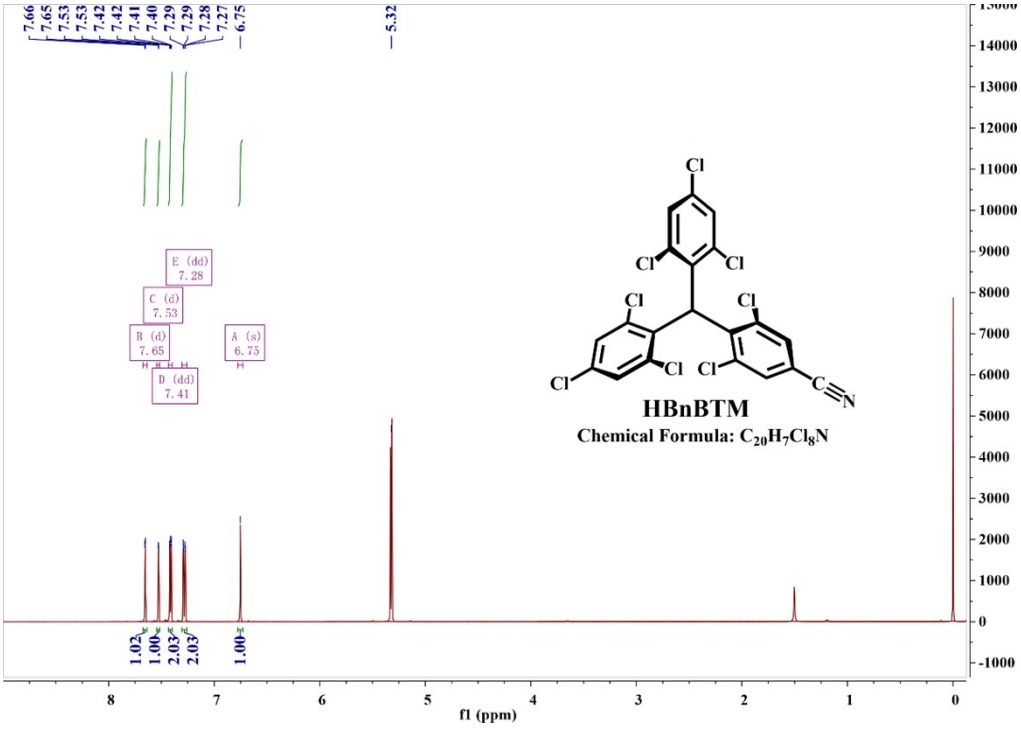

Fig. S1 ^{1}H-NMR spectrum of HBnBTM in CD_2Cl_2.

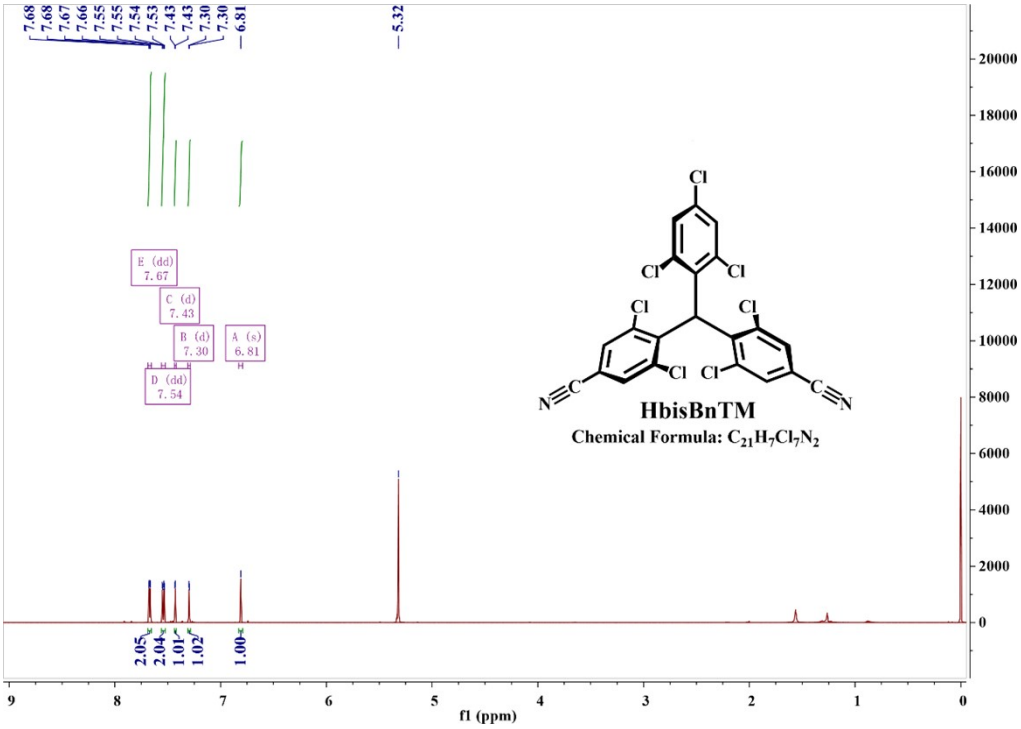

Fig. S2 ^{1}H-NMR spectrum of HbisBnTM in CD_2Cl_2.

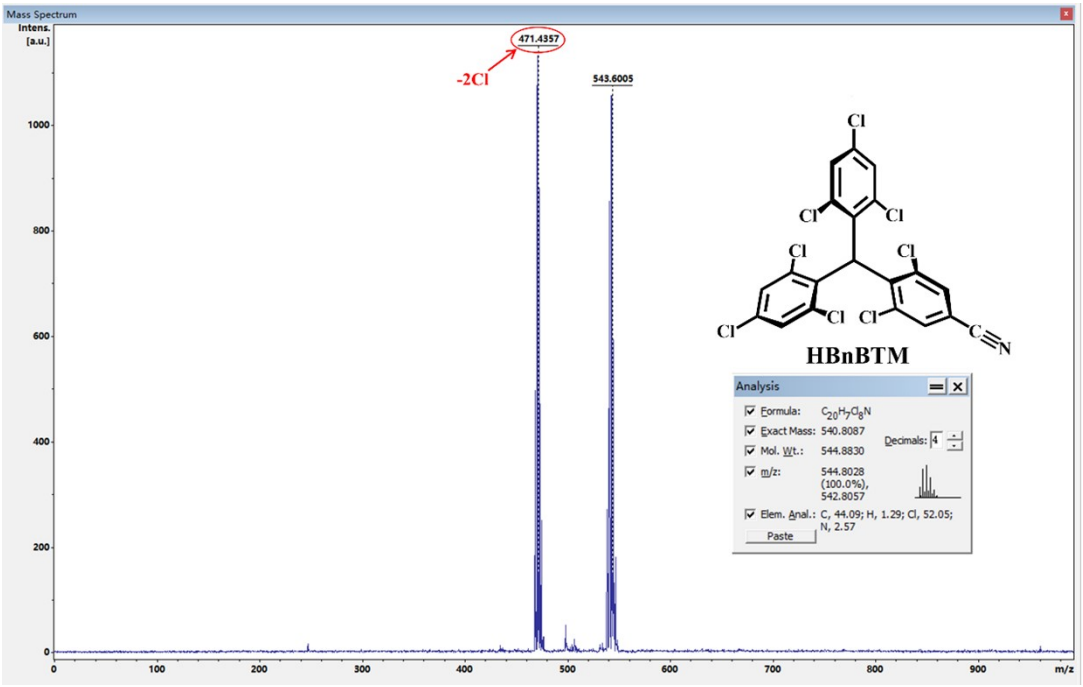

Fig. S3 MALDI-TOF-MS spectrum of HBnBTM.

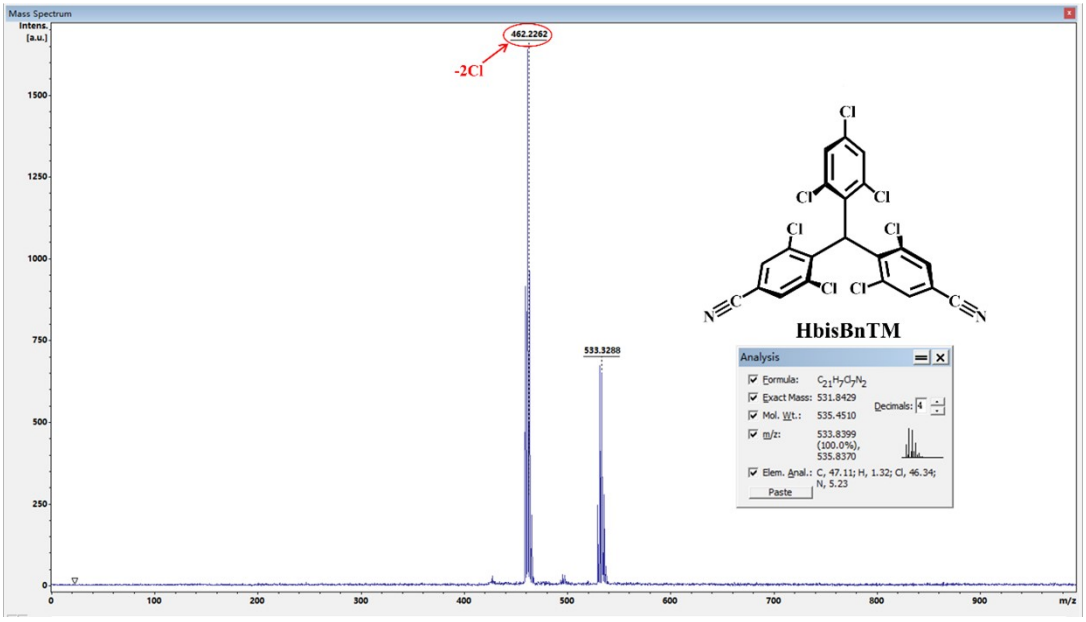

Fig. S4 MALDI-TOF-MS spectrum of HbisBnTM.

(3) Preparation of BnBTM and bisBnTM

Under argon atmosphere and in the dark, HBnBTM (0.54 g, 1.0 mmol) was dissolved in a mixture of dry THF (5.0 ml) and DMF (10.0 ml). Then NaH (0.40g, 60%, 10.00 mmol) was added. The solution was stirred for 5 h in the dark at room temperature, and then p-chloranil (1.23 g, 5.0 mmol) was added. The solution was stirred for further 1 h. After the reaction finished, the solvent was removed under vacuum and the crude product was purified by silica gel column chromatography (using petroleum ether: dichloromethane = 9:1 v/v). The crude product was recrystallized from dichloromethane and methanol. Finally, BnBTM was obtained as a red solid (0.39 g, 72% yield). MALDI-TOF-MS (m/z): calculated for $C_{20}H_6Cl_8N$, 543.7949; found, 542.5274. Elem. Anal. Calcd for $C_{20}H_6Cl_8N$: C 44.17, H 1.11, N 2.58; found, C 44.44, H 1.39, N 2.62.

bisBnTM was obtained by the same method.

Under argon atmosphere and in the dark, HbisBnTM (0.53 g, 1.0 mmol) was dissolved in a mixture of dry THF (5.0 ml) and DMF (10.0 ml). Then NaH (0.40g, 60%, 10.00 mmol) was added. The solution was stirred for 5 h in the dark at room temperature, and then p-chloranil (1.23 g, 5.0 mmol) was added. The solution was stirred for further 1 h. After the reaction finished, the solvent was removed under vacuum and the crude product was purified by silica gel column chromatography (using petroleum ether: dichloromethane = 4:1 v/v). The crude product was recrystallized from dichloromethane and methanol. bisBnTM was obtained as a red solid (0.39 g, 73% yield). MALDI-TOF-MS (m/z): calculated for $C_{21}H_6Cl_7N_2$, 532.8321; found, 532.4715.

Elem. Anal. Calcd for $C_{21}H_6Cl_7N_2$: C 47.20, H 1.13, N 5.24; found, C 47.69, H 1.36, N 5.37.

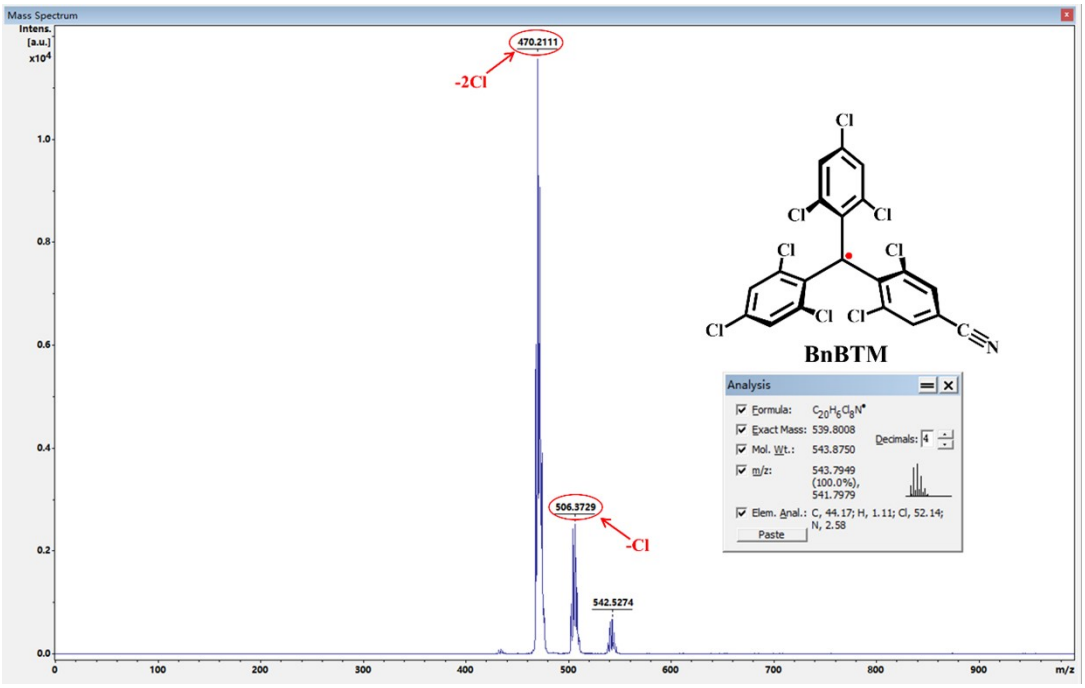

Fig. S4 MALDI-TOF-MS spectrum of BnBTM.

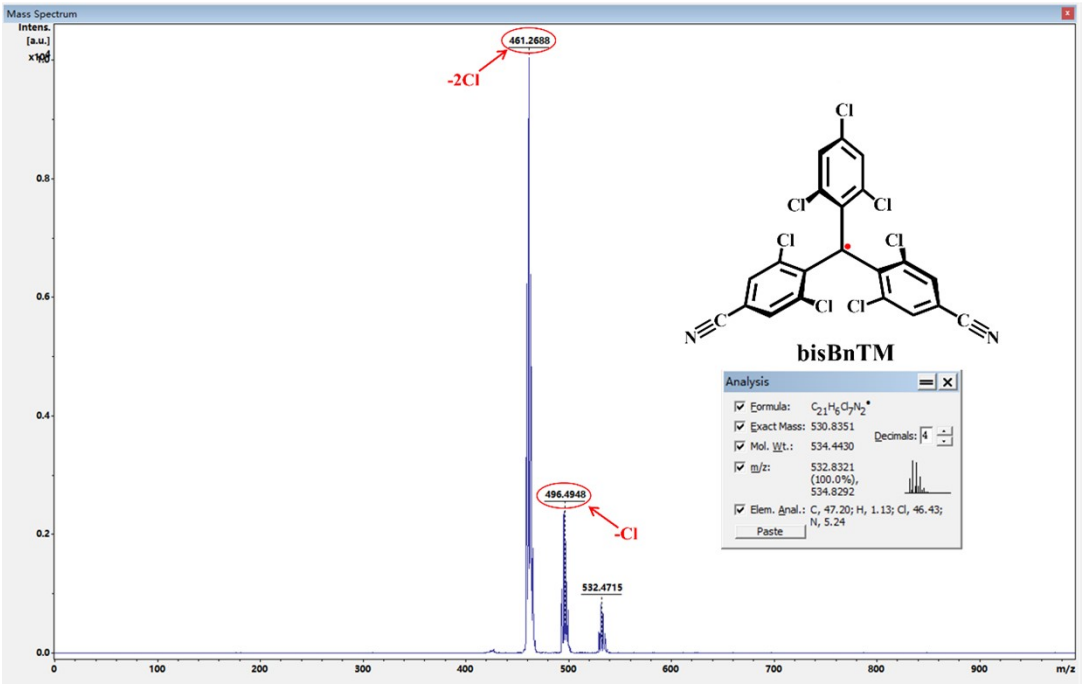

Fig. S6 MALDI-TOF-MS spectrum of bisBnTM.

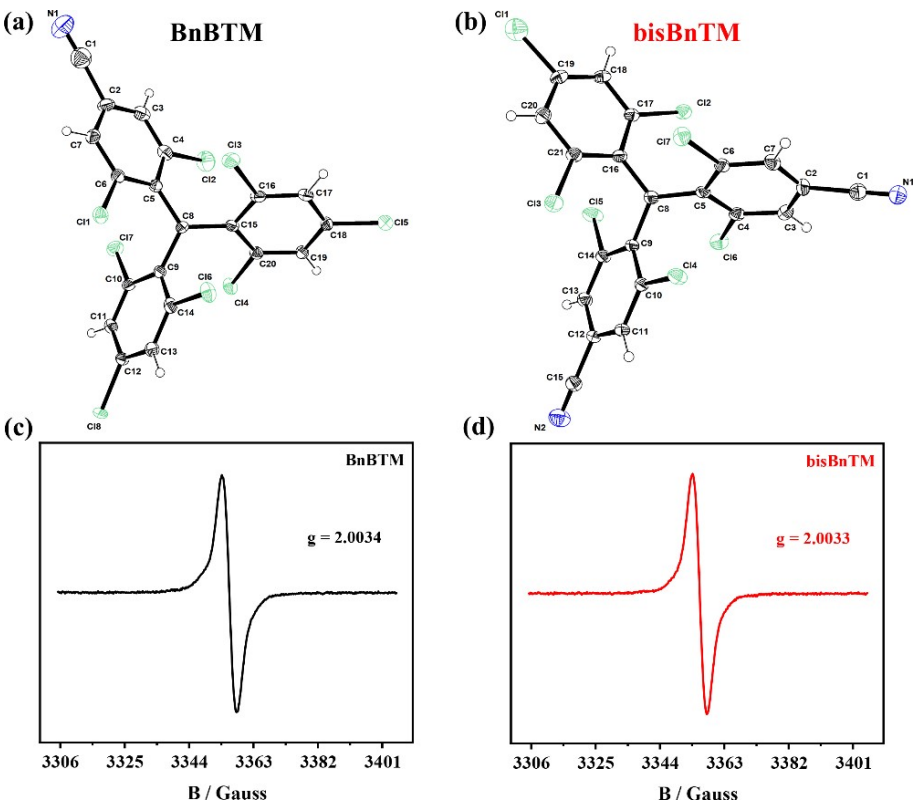

Fig. S7 Crystal structure of (a) BnBTM and (b) bisBnTM with thermal ellipsoids set at50 % probability; EPR spectrum of (c) BnBTM and (d) bisBnTM in in chloroform at room temperature.

Table S1. Crystal data and structure refinement for BnBTM.

Identification code	BnBTM
Empirical formula	$C_{20}H_6Cl_8N$
Formula weight	543.86
Temperature/K	110.00
Crystal system	monoclinic
Space group	$P2_1/c$
a/Å	14.0305(9)
b/Å	8.0731(5)
c/Å	18.9296(12)
α/°	90
β/°	94.608(2)
γ/°	90
Volume/Å^3	2137.2(2)
Z	4
ρ_{calc}g/cm^3	1.690
μ/mm^{-1}	1.063

F(000)	1076.0
Crystal size/mm^3	0.05 × 0.03 × 0.02
Radiation	MoKα (λ = 0.71073)
2Θ range for data collection/°	5.4 to 55.004
Index ranges	-18 ≤ h ≤ 18, -10 ≤ k ≤ 10, -24 ≤ l ≤ 24
Reflections collected	47418
Independent reflections	4910 [R_{int}= 0.0422, R_{sigma}= 0.0213]
Data/restraints/parameters	4910/80/283
Goodness-of-fit on F^2	1.148
Final R indexes [I>=2σ (I)]	R_1= 0.0585, wR_2= 0.1391
Final R indexes [all data]	R_1= 0.0686, wR_2= 0.1459
Largest diff. peak/hole / e Å^{-3}	0.65/-0.80

Table S2. Crystal data and structure refinement for bisBnTM.

Identification code	bisBnTM
Empirical formula	$C_{21}H_6Cl_7N_2$
Formula weight	534.43
Temperature/K	201.00
Crystal system	triclinic
Space group	P-1
a/Å	8.2197(11)
b/Å	11.2036(15)
c/Å	13.6336(18)
α/°	67.189(5)
β/°	84.761(5)
γ/°	73.004(5)
Volume/Å^3	1106.4(3)
Z	2
ρ_{calc}g/cm^3	1.604
μ/mm^{-1}	0.909
F(000)	530.0
Crystal size/mm^3	0.05 × 0.03 × 0.02
Radiation	MoKα (λ = 0.71073)
2Θ range for data collection/°	5.184 to 55.058
Index ranges	-10 ≤ h ≤ 10, -14 ≤ k ≤ 14, -17 ≤ l ≤ 17
Reflections collected	27967
Independent reflections	5069 [R_{int}= 0.0539, R_{sigma}= 0.0363]
Data/restraints/parameters	5069/56/298
Goodness-of-fit on F^2	1.035

Final R indexes [I>=2σ (I)]	R_1= 0.0443, wR_2= 0.1015
Final R indexes [all data]	R_1= 0.0515, wR_2= 0.1067
Largest diff. peak/hole / e Å^{-3}	0.88/-1.28

2. Photophysical parameters of BnBTM and bisBnTM in various solvents

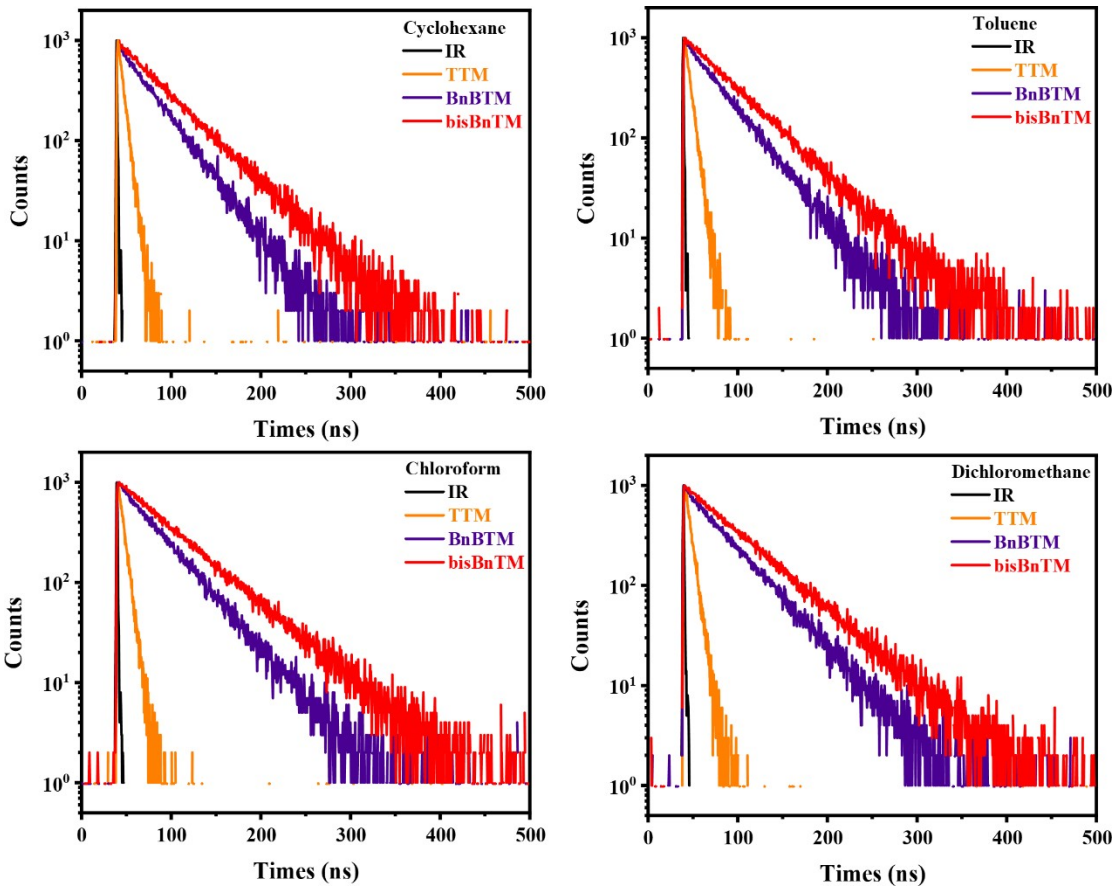

Fig. S8 Transient photoluminescence decay spectra of TTM, BnBTM and bisBnTM in various solvents at room temperature.

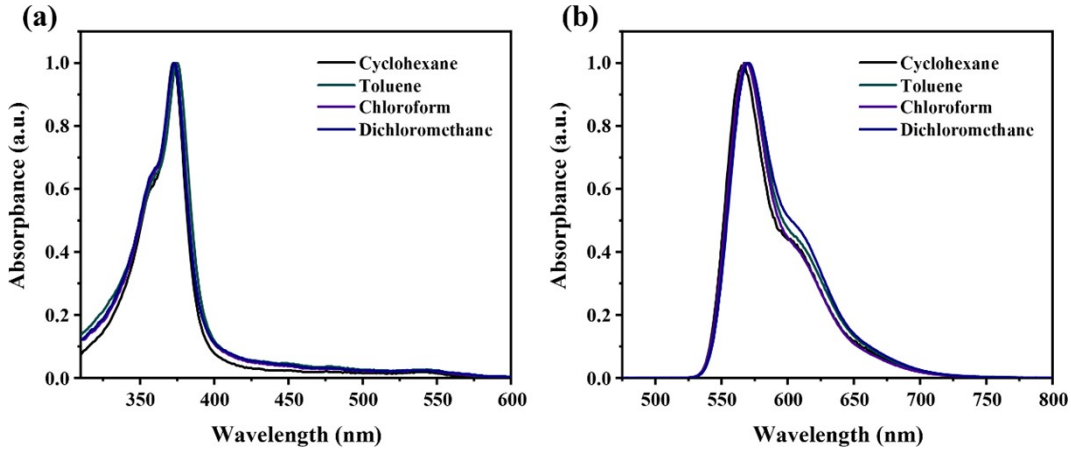

Fig. S9 The normalized UV-vis absorption and PL spectra of TTM in various solvents (10^{-5} M) at room temperature.

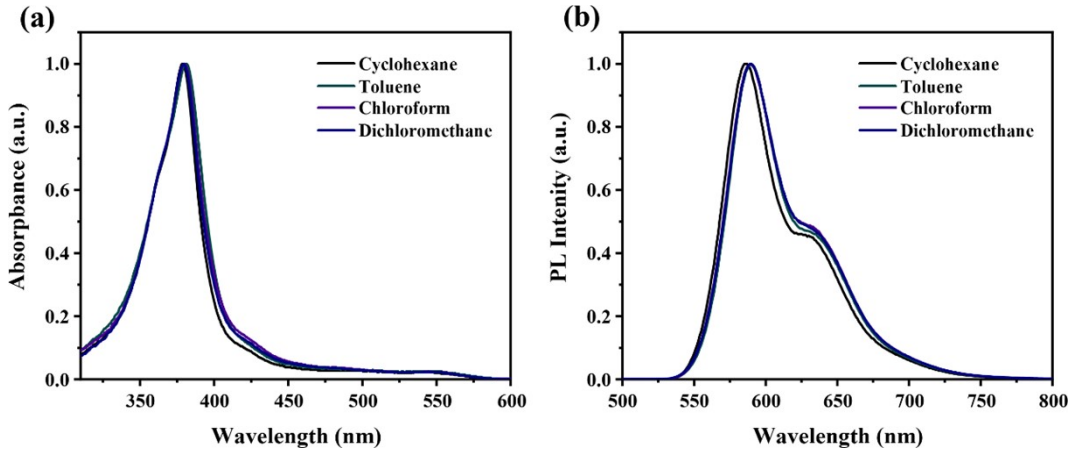

Fig. S10 The normalized UV-vis absorption and PL spectra of BnBTM in various solvents (10^{-5} M) at room temperature.

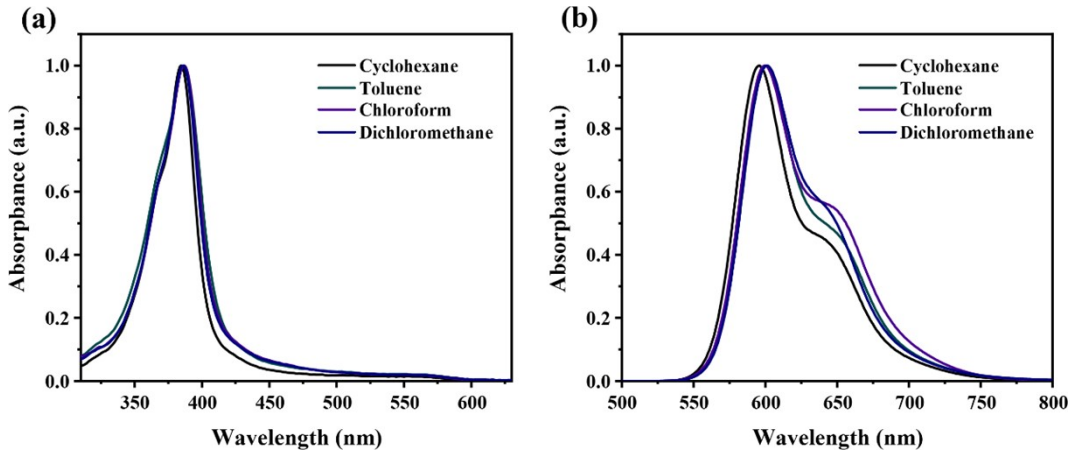

Fig. S11 The normalized UV-vis absorption and PL spectra of bisBnTM in various solvents (10^{-5} M) at room temperature.

Table S3. Photophysical parameters of TTM, BnBTM, and bisBnTM in different solvents.

Radical	Solvent	λ_{abs} [a] (nm)	λ_{PL} [b] (nm)	PLQE [c][d] (%)	t [d] (ns)	k_r [e] 10^6 (s^{-1})	k_{nr} [e] 10^6 (s^{-1})
TTM	Toluene	375/543	570	1.4	5.9	2.4	166.0
	Chloroform	373/543	568	1.7	6.0	2.8	164.7
	Dichloromethane	373/542	570	1.5	6.4	2.4	154.4
BnBTM	Toluene	381/551	590	5.3	37.8	1.4	25.1
	Chloroform	380/552	592	6.5	41.2	1.6	22.7
	Dichloromethane	379/551	587	6.2	42.9	1.4	21.9
bisBnTM	Toluene	387/563	600	10.4	50.9	2.0	17.6
	Chloroform	387/560	600	11.2	56.5	2.0	15.7
	Dichloromethane	386/562	601	10.0	55.7	1.8	16.1

[a] absorption peaks in different solvents. [b] emission peaks in various solvents [c] measured with a calibrated integrating sphere system. [d] measured using Edinburgh fluorescence spectrometer (FLS980) at room temperature. [e] Calculated from the equation: $\phi = k_r/(k_r + k_{nr})$; $\tau = 1/(k_r + k_{nr})$.

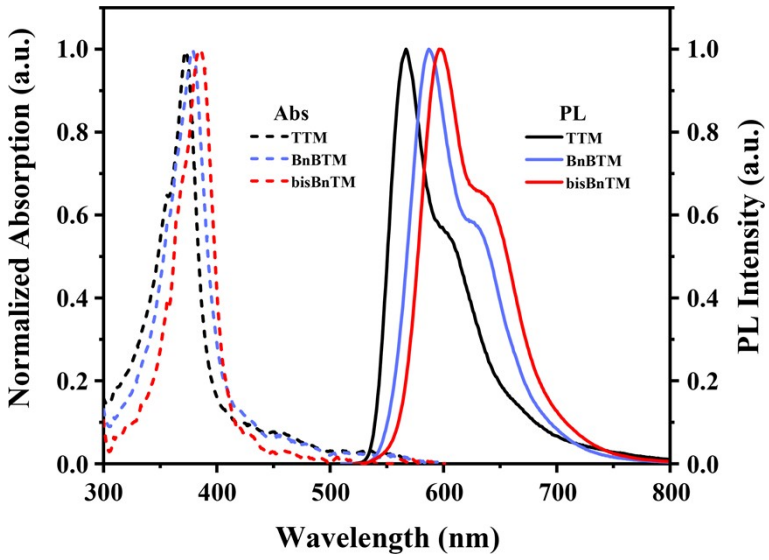

Fig. S12 Normalized UV-vis absorption and PL spectra of TTM, BnBTM and bisBnTM in PMMA film at 3 wt%.

Table S4. Photophysical parameters of TTM, BnBTM and bisBnTM in PMMA film.

Radical	Concentration (wt%)	λ_{abs} [a] (nm)	λ_{PL} [b] (nm)	PLQE [c] (%)
TTM	3	373	567	5.0
BnBTM	3	379	587	9.0
bisBnTM	3	385	596	12.0

[a] absorption peaks in PMMA film. [b] emission peaks in PMMA film. [c] The PLQE was measured with a calibrated integrating sphere system.

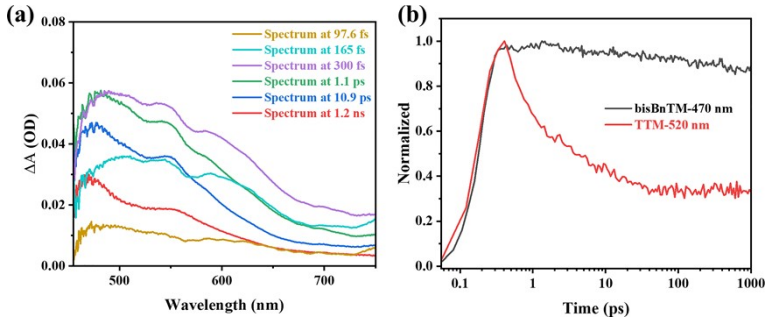

Fig. S13 Transient absorption studies of bisBnTM and TTM. (a) Femtosecond to nanosecond time-slices from transient absorption studies of bisBnTM (375 nm excitation, 1×10^{-4} M in cyclohexane). (b) Kinetic profiles of bisBnTM and TTM (375 nm excitation, 1×10^{-4} M in chloroform). The two curves represent the D_1 excited state dynamics of their respective molecules.

Fig. 13 (a) displays the transient absorption spectra of bisBnTM within the visible light range. Under the excitation of a 375 nm laser pulse, the ground state molecules are rapidly excited to the excited state within 97.6 fs, reaching their peak at around 300 fs. This process is reflected in the excited state absorption (ESA) peaks around 490 and 545 nm. Over time, the peak positions shift towards 470 nm and 558 nm. This indicates that the molecules are initially excited to high-energy localized states, followed by a rapid transition to the first excited state (D_1). Fig. 13(b) compares the D_1 excited-state dynamics of bisBnTM and TTM in chloroform solvent. The D_1 excited state of TTM shows an obviously shorter excited state lifetime. This suggests that the non-radiative transition process of bisBnTM is effectively suppressed compared to that of TTM.

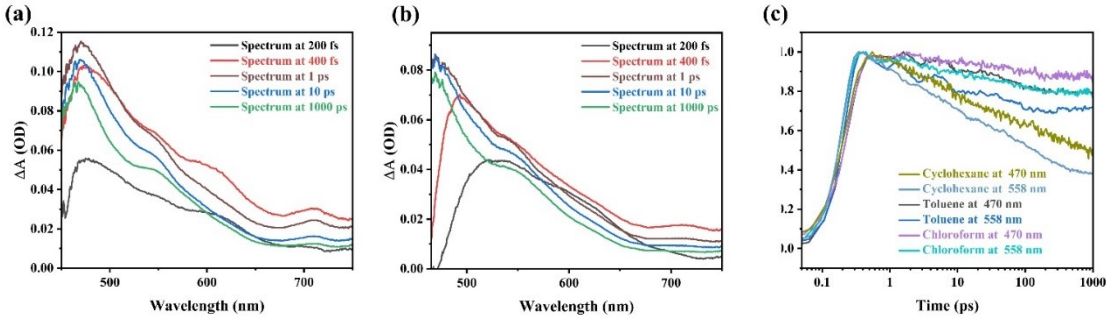

Fig. S14 Femtosecond to nanosecond time-slices from transient absorption studies of bisBnTM in (a) toluene and (b) chloroform (10^{-4} M); (c) kinetic profiles of bisBnTM in those solvents (excited at 375 nm).

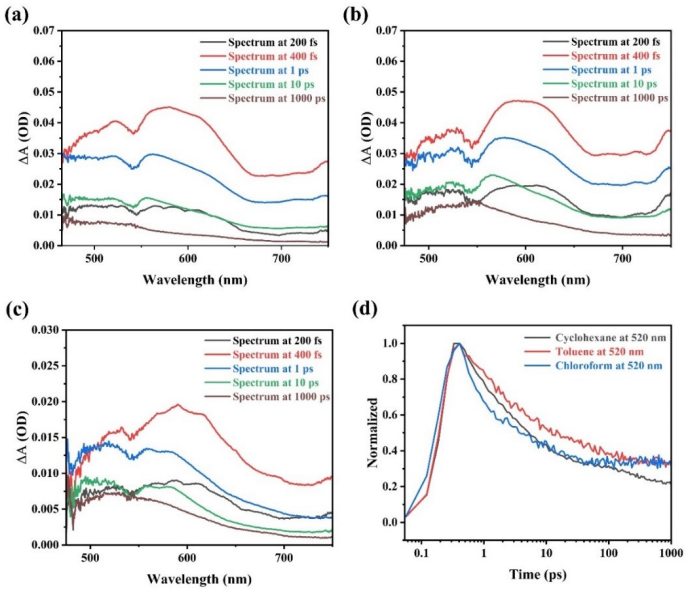

Fig. S15. Femtosecond to nanosecond time-slices from transient absorption studies of TTM in (a) cyclohexane, (b) toluene and (c) chloroform; (d) kinetic profiles of TTM at 520nm in those solvents (excited at 375 nm).

3. Theoretical calculation results.

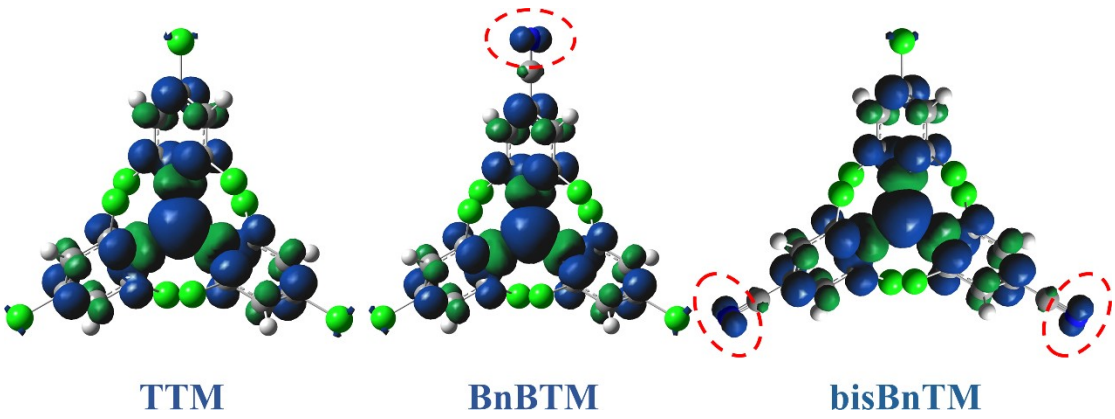

Fig. S16 Spin density distribution of TTM, BnBTM and bisBnTM by DFT calculations (isovalue =0.0015).

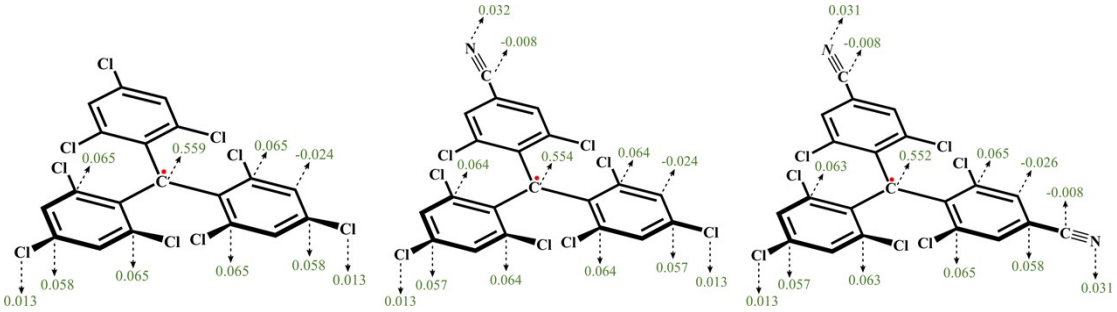

Fig. S17 Spin densities of the optimized geometries of TTM, BnBTM, and bisBnTM (calculated by Multiwfn at Becke mode).[4]

Table S5. Spin densities of the optimized geometries of TTM, BnBTM, and bisBnTM

TTM		BnBTM		bisBnTM	
Atomic space	Spin population	Atomic space	Spin population	Atomic space	Spin population
1(C)	0.065	1(C)	0.064	1(C)	0.065
2(C)	-0.030	2(C)	-0.029	2(C)	-0.033
3(C)	0.065	3(C)	0.064	3(C)	0.065
4(C)	-0.024	4(C)	-0.024	4(C)	-0.026
5(C)	0.058	5(C)	0.057	5(C)	0.058
6(C)	-0.024	6(C)	-0.024	6(C)	-0.026
7(H)	0.001	7(H)	0.001	7(H)	0.001
8(H)	0.001	8(H)	0.001	8(H)	0.001
9(C)	0.559	9(C)	0.554	9(C)	0.552
10(C)	-0.030	10(C)	-0.033	10(C)	-0.033
11(C)	0.065	11(C)	0.066	11(C)	0.065
12(C)	0.065	12(C)	0.066	12(C)	0.065
13(C)	-0.024	13(C)	-0.027	13(C)	-0.026
14(C)	-0.024	14(C)	-0.027	14(C)	-0.026
15(C)	0.058	15(C)	0.060	15(C)	0.058
16(H)	0.001	16(H)	0.001	16(H)	0.001
17(H)	0.001	17(H)	0.001	17(H)	0.001
18(C)	-0.030	18(C)	-0.029	18(C)	-0.029
19(C)	0.065	19(C)	0.064	19(C)	0.063
20(C)	0.065	20(C)	0.064	20(C)	0.063
21(C)	-0.024	21(C)	-0.024	21(C)	-0.023
22(C)	-0.024	22(C)	-0.024	22(C)	-0.023
23(C)	0.058	23(C)	0.057	23(C)	0.057
24(H)	0.001	24(H)	0.001	24(H)	0.001

25(H)	0.001	25(H)	0.001	25(H)	0.001
26(Cl)	0.012	26(Cl)	0.012	26(Cl)	0.012
27(Cl)	0.012	27(Cl)	0.011	27(Cl)	0.012
28(Cl)	0.013	28(Cl)	0.013	28(Cl)	0.013
29(Cl)	0.012	29(Cl)	0.011	29(Cl)	0.013
30(Cl)	0.012	30(Cl)	0.012	30(Cl)	0.013
31(Cl)	0.013	31(Cl)	0.013	31(Cl)	0.013
32(Cl)	0.012	32(Cl)	0.012	32(Cl)	0.012
33(Cl)	0.012	33(Cl)	0.012	33(C)	-0.008
34(Cl)	0.013	34(C)	-0.008	34(N)	0.031
		35(N)	0.032	35(C)	-0.008
				36(N)	0.031

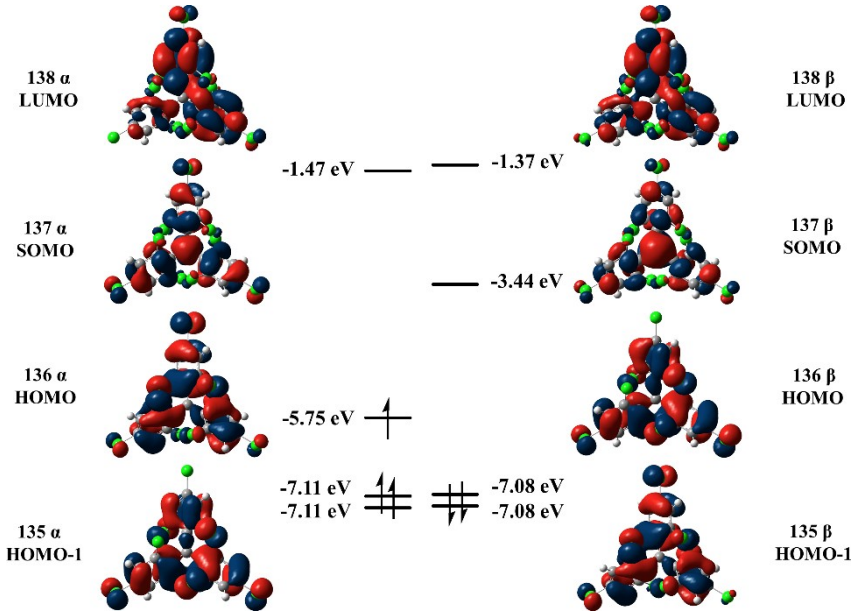

Fig. S18 Ground-state frontier orbitals of TTM from DFT calculations (UB3LYP/6-31G(d,p)).

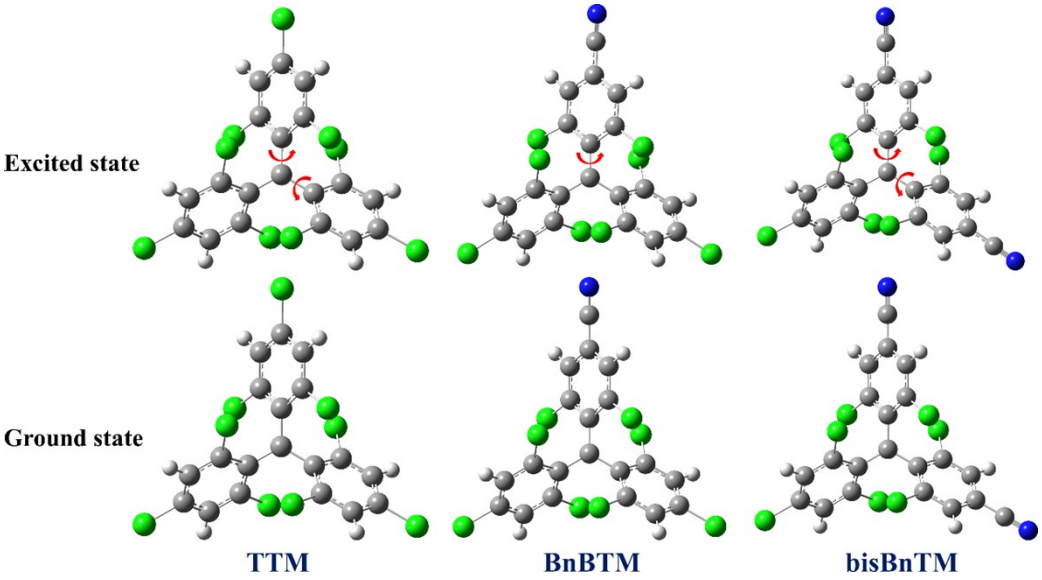

Fig. S19 Geometries of TTM, BnBTM and bisBnTM at ground state and optimized excited state by DFT and TD-DFT calculations (UB3LYP/6-31G(d,p)).

Table S6. Dihedral angles of TTM, BnBTM and bisBnTM radicals in their DFT calculated D_0 and D_1 geometries. *A*, *B* and *C* refer to the dihedrals between the center plane of the carbon radical and the peripheral benzene ring.

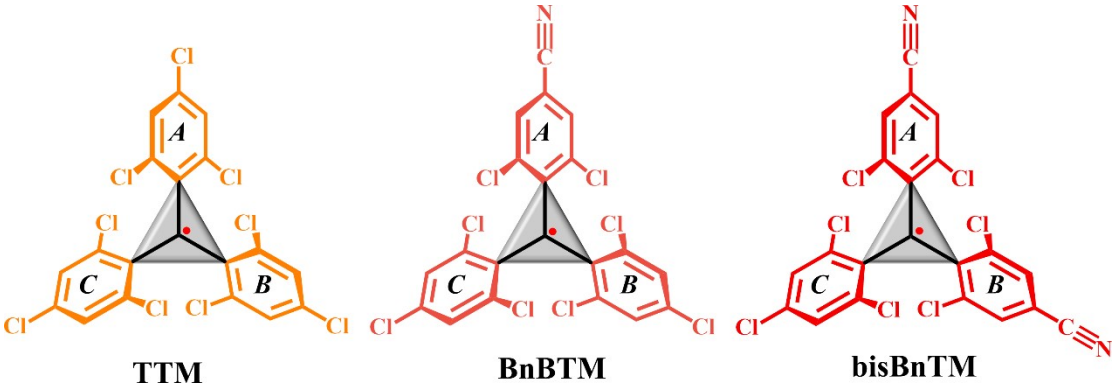

radical	state	*A* (°)	*B* (°)	*C* (°)
TTM	D_1	**43.0**	**42.1**	46.6
	D_0	48.9	48.8	48.8
BnBTM	D_1	**35.4**	47.6	47.0
	D_0	48.4	48.7	48.9
bisBnTM	D_1	**40.8**	**38.0**	**51.7**
	D_0	48.6	48.5	48.6

4. Electrochemical properties and TGA curve

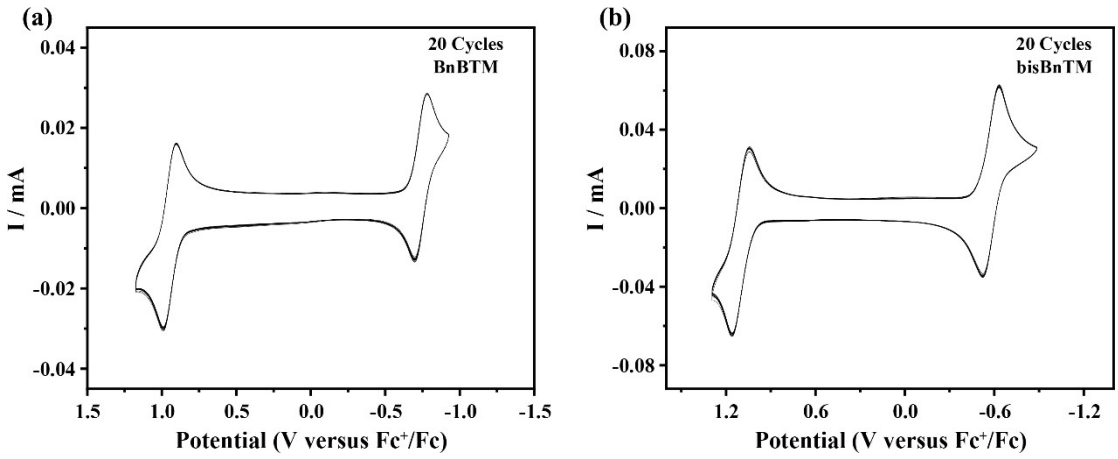

Fig. S20 Multi-cycle CV measurements (20 cycles) of BnBTM and bisBnTM in DCM.

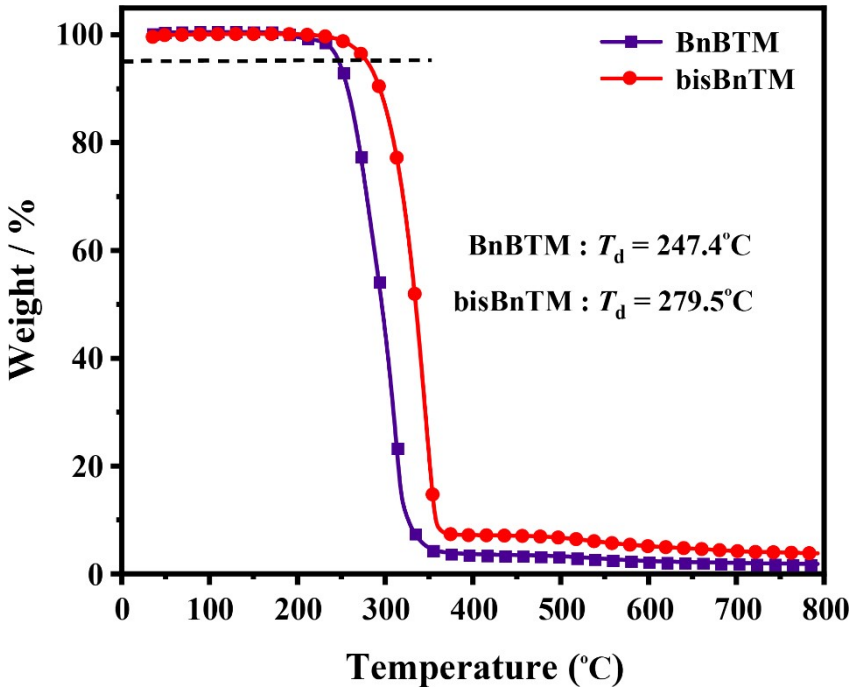

Fig. S21 TGA thermograph of BnBTM and bisBnTM recorded under nitrogen at a heating rate of 10℃/min.

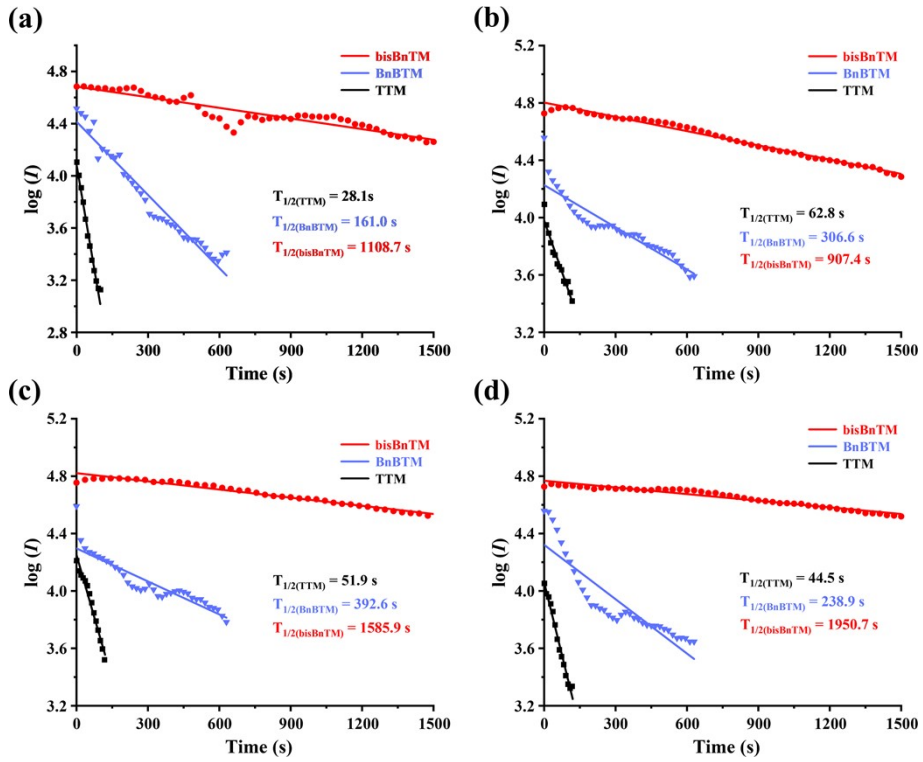

Fig. S22 The fluorescence decay of TTM, BnBTM, and bisBnTM in (a) cyclohexane, (b) toluene, (c) chloroform, and (d) dichloromethane (5×10^{-5}M) under continuous excitation (measured by the RF-6000 Spectro-fluorophotometer with temporal measurement mode; power density: 50 mW cm^{-2}).

5. Extracted results of TD-DFT calculations

Table S7. Excited states of TTM, BnBTM, and bisBnTM calculated by TD-DFT calculations.

TTM (UB3LYP/6-31G(d,p))

Excitation energies and oscillator strengths:

Excited State 1: 2.215-A 2.6555 eV 466.89 nm f=0.0223 <S**2>=0.976

137A ->138A -0.19671

137A ->139A 0.23171

133B ->137B 0.23015

135B ->137B -0.17750

136B ->137B 0.86437

This state for optimization and/or second-order correction.

Total Energy, E(TD-HF/TD-KS) = -4869.25503157

Copying the excited state density for this state as the 1-particle RhoCI density.

Excited State 2: 2.215-A 2.6558 eV 466.85 nm f=0.0223 <S**2>=0.976

137A ->138A 0.23153
137A ->139A 0.19648
132B ->137B 0.22996
135B ->137B 0.86450
136B ->137B 0.17759

Excited State 3: 2.100-A 2.9287 eV 423.34 nm f=0.0065 <S**2>=0.853
137A ->140A 0.15483
133B ->137B 0.19130
134B ->137B 0.94717

Excited State 4: 2.126-A 2.9295 eV 423.22 nm f=0.0029 <S**2>=0.880
137A ->138A -0.17467
132B ->137B -0.28120
133B ->137B 0.83904
134B ->137B -0.16734
135B ->137B 0.17417
136B ->137B -0.27298

Excited State 5: 2.126-A 2.9297 eV 423.19 nm f=0.0029 <S**2>=0.880
137A ->138A 0.10136
137A ->139A 0.17198
132B ->137B 0.84768
133B ->137B 0.25715
134B ->137B -0.16104
135B ->137B -0.27837
136B ->137B -0.16602

Excited State 6: 2.357-A 3.0873 eV 401.60 nm f=0.0000 <S**2>=1.138
135A ->139A -0.13747
136A ->138A 0.13739
137A ->146A -0.24505
131B ->137B 0.87166
134B ->140B 0.10801

Excited State 7: 2.371-A 3.3456 eV 370.59 nm f=0.1795 <S**2>=1.156
133A ->140A -0.10479
134A ->142A 0.12022
137A ->138A 0.77599
137A ->139A 0.18288
131B ->138B 0.10886
132B ->137B -0.28236
133B ->137B 0.15925
135B ->137B -0.28595

135B ->138B -0.10462
136B ->139B 0.10420

Excited State 8: 2.371-A 3.3460 eV 370.54 nm f=0.1799 <S**2>=1.156
132A ->140A 0.10469
134A ->141A -0.12057
137A ->138A -0.18299
137A ->139A 0.77595
131B ->139B 0.10894
132B ->137B -0.15923
133B ->137B -0.28202
135B ->139B 0.10430
136B ->137B -0.28620
136B ->138B 0.10442

Excited State 9: 2.206-A 3.5834 eV 345.99 nm f=0.0110 <S**2>=0.966
137A ->140A 0.95748
134B ->137B -0.17194

Excited State 10: 3.250-A 3.6826 eV 336.68 nm f=0.0000 <S**2>=2.390
132A ->138A 0.12501
132A ->139A 0.11247
132A ->141A -0.20880
133A ->138A -0.11272
133A ->139A 0.12504
133A ->142A -0.20895
134A ->140A 0.32063
135A ->139A 0.15893
135A ->142A 0.18339
136A ->138A -0.15923
136A ->141A -0.18331
131B ->137B 0.40785
131B ->146B 0.11784
132B ->138B -0.14337
132B ->141B 0.18726
133B ->139B -0.14330
133B ->142B 0.18752
134B ->140B -0.29022
135B ->138B -0.20390
135B ->141B -0.16263
136B ->139B -0.20374
136B ->142B -0.16269

Excited State 11: 2.329-A 3.7700 eV 328.87 nm f=0.0057 <S**2>=1.106

133A ->140A -0.11991
137A ->138A -0.14751
137A ->141A 0.91082
132B ->137B 0.10256
133B ->140B 0.11478

Excited State 12: 2.330-A 3.7705 eV 328.83 nm f=0.0056 <S**2>=1.107
132A ->140A 0.12020
137A ->139A -0.14801
137A ->142A 0.91053
132B ->140B -0.11506
133B ->137B 0.10229

Excited State 13: 3.158-A 3.8750 eV 319.96 nm f=0.0135 <S**2>=2.243
132A ->141A -0.11339
132A ->142A 0.15433
133A ->140A 0.26471
133A ->141A 0.15440
133A ->142A 0.11400
134A ->142A -0.28381
135A ->139A 0.14885
135A ->140A -0.21369
136A ->138A 0.14915
137A ->138A 0.31430
137A ->139A 0.25201
137A ->141A 0.22953
132B ->141B 0.11742
132B ->142B -0.15191
133B ->140B -0.27849
133B ->141B -0.15169
133B ->142B -0.11815
134B ->141B -0.10191
134B ->142B 0.28635
135B ->138B 0.11506
136B ->139B -0.11479
136B ->140B 0.20942

Excited State 14: 3.158-A 3.8754 eV 319.93 nm f=0.0135 <S**2>=2.243
132A ->140A -0.26441
132A ->141A 0.15512
132A ->142A 0.11354
133A ->141A 0.11266
133A ->142A -0.15471
134A ->141A 0.28423

135A ->138A 0.14900
136A ->139A -0.14863
136A ->140A -0.21385
137A ->138A -0.25169
137A ->139A 0.31403
137A ->142A 0.23044
132B ->140B 0.27795
132B ->141B -0.15239
132B ->142B -0.11753
133B ->141B -0.11643
133B ->142B 0.15227
134B ->141B -0.28712
134B ->142B -0.10100
135B ->139B -0.11452
135B ->140B -0.20967
136B ->138B -0.11491

Excited State 15: 3.309-A 4.3037 eV 288.09 nm f=0.0000 <S**2>=2.488
132A ->141A -0.18871
133A ->142A -0.18909
134A ->140A 0.27021
135A ->138A 0.12461
135A ->139A -0.29207
135A ->142A 0.10004
136A ->138A 0.29319
136A ->139A 0.12416
137A ->146A -0.19575
126B ->137B 0.29313
131B ->137B -0.11368
132B ->141B 0.18847
133B ->142B 0.18888
134B ->140B -0.27403
135B ->138B 0.31331
135B ->139B 0.11194
136B ->138B -0.11253
136B ->139B 0.31257

BnBTM (UB3LYP/6-31G(d,p))

Excitation energies and oscillator strengths:

Excited State 1: 2.170-A 2.5726 eV 481.94 nm f=0.0289 <S**2>=0.927
135A ->137A 0.23896
132B ->135B -0.12573
134B ->135B 0.92385
This state for optimization and/or second-order correction.

Total Energy, E(TD-HF/TD-KS) = -4501.90357632
Copying the excited state density for this state as the 1-particle RhoCI density.

Excited State 2:	2.294-A	2.5737 eV	481.73 nm	f=0.0054	<S**2>=1.066
130A ->136A	0.11034				
135A ->136A	-0.43935				
129B ->135B	-0.15617				
129B ->136B	0.12173				
131B ->135B	-0.43639				
133B ->135B	0.70334				

Excited State 3:	2.132-A	2.8103 eV	441.17 nm	f=0.0005	<S**2>=0.887
135A ->136A	0.29900				
129B ->135B	0.14118				
131B ->135B	0.63781				
133B ->135B	0.66234				

Excited State 4:	2.094-A	2.8212 eV	439.48 nm	f=0.0070	<S**2>=0.846
135A ->138A	-0.10361				
132B ->135B	0.96310				
134B ->135B	0.16570				

Excited State 5:	2.169-A	2.8664 eV	432.54 nm	f=0.0082	<S**2>=0.927
135A ->137A	0.14812				
130B ->135B	0.95099				
134B ->135B	-0.13216				

Excited State 6:	2.288-A	2.9724 eV	417.12 nm	f=0.0547	<S**2>=1.058
130A ->136A	-0.16693				
133A ->136A	0.10872				
134A ->137A	0.11465				
135A ->136A	0.36305				
135A ->142A	0.10688				
135A ->143A	-0.15555				
129B ->135B	0.66185				
131B ->135B	-0.48045				
131B ->136B	-0.13174				
133B ->135B	0.12208				

Excited State 7:	2.269-A	3.1861 eV	389.15 nm	f=0.1891	<S**2>=1.037
134A ->137A	-0.11292				
135A ->136A	0.69106				
135A ->143A	0.12916				
129B ->135B	-0.48577				

131B ->135B -0.35285
133B ->135B 0.13575
134B ->137B 0.11378

Excited State 8: 2.544-A 3.3508 eV 370.01 nm f=0.1449 <S**2>=1.369
132A ->140A 0.16954
133A ->138A -0.12295
135A ->137A 0.77868
129B ->137B -0.10009
130B ->135B -0.20249
131B ->137B 0.11846
132B ->135B 0.12206
132B ->140B -0.13717
133B ->137B -0.10732
133B ->138B -0.10593
134B ->135B -0.27998
134B ->136B 0.14759
134B ->144B -0.10055

Excited State 9: 3.163-A 3.6360 eV 340.99 nm f=0.0014 <S**2>=2.252
130A ->136A 0.26771
130A ->140A -0.12405
131A ->137A 0.12134
131A ->138A -0.15573
131A ->139A 0.18579
132A ->138A 0.22766
133A ->136A -0.18139
133A ->140A -0.19684
134A ->137A -0.15052
134A ->139A 0.14956
129B ->135B 0.46158
129B ->136B 0.14936
129B ->144B 0.10418
130B ->137B 0.11918
130B ->138B -0.14156
130B ->139B 0.16845
131B ->136B 0.27772
131B ->140B -0.11654
132B ->138B -0.20423
133B ->136B -0.22572
133B ->140B -0.17213
134B ->137B 0.19354
134B ->139B -0.13466

Excited State 10:	2.206-A	3.6442 eV	340.22 nm	f=0.0093	<S**2>=0.967
135A ->138A	0.95750				
132B ->135B	0.11992				

Excited State 11:	3.264-A	3.7630 eV	329.48 nm	f=0.0057	<S**2>=2.414
129A ->136A	0.15810				
130A ->136A	0.13996				
130A ->140A	0.14867				
131A ->138A	-0.25373				
131A ->139A	0.19915				
132A ->138A	-0.15934				
132A ->139A	-0.21750				
133A ->136A	-0.19140				
133A ->140A	0.21903				
134A ->137A	0.22189				
134A ->138A	-0.12971				
135A ->136A	0.28381				
135A ->140A	-0.14635				
135A ->143A	-0.10342				
129B ->136B	0.22563				
130B ->138B	-0.26765				
130B ->139B	0.20865				
131B ->135B	0.12348				
131B ->140B	0.14812				
132B ->137B	0.10656				
132B ->138B	0.15290				
132B ->139B	0.21396				
133B ->135B	-0.10755				
133B ->136B	-0.10432				
133B ->140B	0.21070				
134B ->137B	-0.21160				
134B ->138B	0.12050				

Excited State 12:	2.428-A	3.8190 eV	324.65 nm	f=0.0113	<S**2>=1.224
130A ->138A	0.15340				
132A ->140A	-0.10945				
134A ->136A	0.12320				
134A ->140A	-0.12636				
135A ->137A	0.29445				
135A ->139A	0.83159				
131B ->138B	0.14473				
132B ->140B	0.11433				
134B ->140B	0.12816				

Excited State 13:	2.358-A	3.8435 eV	322.58 nm	f=0.0015	<S**2>=1.140
134A ->138A	-0.14598				
135A ->140A	0.92039				
131B ->135B	0.10171				
132B ->137B	-0.11293				
134B ->138B	0.13945				

Excited State 14:	2.979-A	3.8947 eV	318.34 nm	f=0.0158	<S**2>=1.969
130A ->138A	-0.10365				
130A ->139A	-0.15498				
132A ->140A	0.31298				
133A ->138A	-0.27041				
133A ->139A	-0.15629				
134A ->136A	-0.17611				
135A ->137A	-0.40192				
135A ->139A	0.43752				
128B ->135B	-0.13322				
131B ->138B	-0.12917				
131B ->139B	-0.15467				
132B ->140B	-0.31930				
133B ->137B	-0.10219				
133B ->138B	-0.26631				
133B ->139B	-0.15981				
134B ->136B	0.14402				

Excited State 15:	3.390-A	4.0930 eV	302.92 nm	f=0.0021	<S**2>=2.623
131A ->136A	0.63089				
132A ->136A	-0.19562				
134A ->136A	0.31870				
130B ->135B	0.13971				
130B ->136B	0.52646				
132B ->136B	0.15280				
134B ->136B	-0.24290				

---

bisBnTM (UB3LYP/6-31G(d,p))

Excitation energies and oscillator strengths:

Excited State 1:	2.187-A	2.5126 eV	493.46 nm	f=0.0250	<S**2>=0.946
133A ->135A	0.25623				
129B ->133B	0.14634				
132B ->133B	0.91610				

This state for optimization and/or second-order correction.

Total Energy, E(TD-HF/TD-KS) = -4134.55082329

Copying the excited state density for this state as the 1-particle RhoCI density.

Excited State 2:	2.299-A	2.5252 eV	490.98 nm	f=0.0033	<S**2>=1.071
133A ->134A	0.44614				
127B ->134B	0.12439				
128B ->133B	0.49624				
130B ->133B	0.27093				
131B ->133B	0.62082				
Excited State 3:	2.119-A	2.7191 eV	455.97 nm	f=0.0021	<S**2>=0.872
133A ->134A	-0.25188				
128B ->133B	-0.42164				
130B ->133B	-0.40424				
131B ->133B	0.74575				
Excited State 4:	2.145-A	2.7695 eV	447.67 nm	f=0.0065	<S**2>=0.900
133A ->134A	-0.16567				
128B ->133B	-0.44684				
130B ->133B	0.84153				
131B ->133B	0.13966				
Excited State 5:	2.162-A	2.7817 eV	445.71 nm	f=0.0062	<S**2>=0.919
133A ->135A	0.18105				
129B ->133B	0.92563				
132B ->133B	-0.23122				
Excited State 6:	2.442-A	2.9356 eV	422.35 nm	f=0.0150	<S**2>=1.241
128A ->134A	-0.21209				
131A ->134A	-0.11397				
132A ->135A	-0.14173				
133A ->135A	0.29880				
133A ->139A	-0.20278				
127B ->133B	0.76599				
128B ->134B	0.17652				
129B ->133B	-0.19146				
132B ->133B	-0.15787				
Excited State 7:	2.108-A	3.0886 eV	401.43 nm	f=0.2522	<S**2>=0.861
133A ->134A	0.77344				
125B ->133B	0.10943				
128B ->133B	-0.57147				
130B ->133B	-0.12554				
131B ->133B	-0.11044				
Excited State 8:	2.444-A	3.2756 eV	378.51 nm	f=0.1558	<S**2>=1.243

131A ->138A 0.15486
132A ->135A 0.11702
133A ->135A 0.76206
133A ->139A 0.17719
127B ->133B -0.30323
129B ->133B -0.21304
131B ->138B -0.12934
132B ->133B -0.23697
132B ->135B -0.16078

Excited State 9: 3.138-A 3.5833 eV 346.00 nm f=0.0001 <S**2>=2.212
128A ->134A 0.29136
129A ->135A 0.13223
129A ->137A -0.18298
130A ->136A 0.23252
131A ->134A 0.15555
131A ->138A 0.17946
132A ->135A 0.17596
132A ->137A 0.13943
127B ->133B 0.48082
127B ->135B -0.11410
127B ->140B 0.11286
128B ->134B -0.33651
129B ->135B -0.12430
129B ->137B 0.17251
130B ->134B -0.12094
130B ->136B -0.20969
131B ->134B -0.18453
131B ->138B -0.15865
132B ->135B -0.21830
132B ->137B -0.12002

Excited State 10: 2.399-A 3.7098 eV 334.21 nm f=0.0073 <S**2>=1.189
129A ->136A -0.10696
130A ->137A 0.12774
132A ->134A -0.14201
133A ->134A -0.12063
133A ->136A 0.88052
127B ->134B 0.11239
130B ->133B -0.12246
130B ->137B -0.12814
131B ->135B 0.12304

Excited State 11: 3.116-A 3.7108 eV 334.12 nm f=0.0089 <S**2>=2.178

127A ->134A 0.17592
128A ->135A 0.16573
128A ->137A 0.15838
129A ->136A 0.22380
130A ->135A 0.10206
130A ->137A -0.22569
131A ->135A 0.13687
132A ->134A 0.27791
132A ->136A -0.14301
132A ->138A -0.10452
133A ->134A 0.27538
133A ->136A 0.37346
125B ->133B -0.10799
127B ->134B -0.24436
128B ->133B 0.15160
128B ->135B -0.16743
128B ->137B -0.16113
129B ->136B -0.24536
130B ->137B 0.23502
132B ->134B -0.24204
132B ->136B 0.12550
132B ->138B 0.10362

Excited State 12: 3.139-A 3.8019 eV 326.11 nm f=0.0203 <S**2>=2.213
127A ->135A 0.11287
128A ->134A 0.12848
128A ->136A -0.15023
129A ->137A -0.11166
130A ->138A 0.20774
131A ->134A 0.17920
131A ->136A 0.23846
131A ->138A -0.32086
132A ->135A -0.17269
132A ->139A -0.10457
133A ->135A 0.42560
133A ->137A -0.17128
127B ->135B -0.10996
128B ->134B -0.10391
128B ->136B 0.15552
129B ->137B 0.14388
130B ->138B -0.20523
131B ->134B -0.10764
131B ->136B -0.23467
131B ->138B 0.32397

132B ->135B	0.19681				
Excited State 13:	2.348-A	3.8987 eV	318.01 nm	f=0.0003	<S**2>=1.128
131A ->136A	0.10671				
133A ->137A	0.90144				
129B ->133B	0.12814				
130B ->134B	-0.20981				
131B ->136B	-0.10651				
Excited State 14:	2.379-A	3.9035 eV	317.62 nm	f=0.0016	<S**2>=1.165
132A ->136A	-0.13621				
133A ->138A	0.90979				
129B ->134B	0.12532				
130B ->135B	0.11076				
131B ->135B	-0.13526				
132B ->136B	0.13062				
132B ->138B	-0.10809				
Excited State 15:	3.394-A	4.0259 eV	307.97 nm	f=0.0014	<S**2>=2.630
128A ->135A	-0.11589				
129A ->134A	0.49757				
130A ->135A	0.28901				
130A ->139A	-0.10081				
132A ->134A	-0.40624				
133A ->138A	0.12882				
129B ->134B	-0.44776				
130B ->133B	0.12003				
130B ->135B	-0.22283				
132B ->134B	0.31741				

Table S8. Optimized excited states of BnBTM and bisBnTM calculated by TD-DFT calculations.

BnBTM (UB3LYP/6-31G(d,p))

Excited State 1:	2.120-A	2.0962 eV	591.46 nm	f=0.0270	<S**2>=0.873
135A ->136A	0.19125				
135A ->137A	0.12686				
134B ->135B	-0.94928				

This state for optimization and/or second-order correction.

Total Energy, E(TD-HF/TD-KS) = -4501.91166398

Copying the excited state density for this state as the 1-particle RhoCI density.

Excited State 2:	2.151-A	2.3540 eV	526.70 nm	f=0.0234	<S**2>=0.907

135A ->136A 0.28699
135A ->137A -0.15242
129B ->135B 0.11910
131B ->135B -0.17141
133B ->135B -0.88380
134B ->135B 0.10823

Excited State 3: 2.087-A 2.5499 eV 486.24 nm f=0.0091 <S**2>=0.839
135A ->138A -0.10535
130B ->135B -0.18351
132B ->135B 0.95602

Excited State 4: 2.109-A 2.6474 eV 468.33 nm f=0.0002 <S**2>=0.862
135A ->136A -0.32795
129B ->135B -0.15913
130B ->135B 0.11001
131B ->135B 0.83361
132B ->135B -0.10293
133B ->135B -0.31634
134B ->135B -0.10784

Excited State 5: 2.128-A 2.7072 eV 457.98 nm f=0.0062 <S**2>=0.882
135A ->137A -0.15702
135A ->139A -0.10334
130B ->135B -0.92414
131B ->135B 0.13540
132B ->135B -0.20283

Excited State 6: 2.165-A 2.8451 eV 435.79 nm f=0.0882 <S**2>=0.922
131A ->136A 0.10338
133A ->136A 0.10161
135A ->136A 0.52163
127B ->135B -0.10251
129B ->135B 0.61341
130B ->135B 0.10404
131B ->135B 0.41766
133B ->135B 0.17776
134B ->135B 0.11023

BisBnTM (UB3LYP/6-31G(d,p))

Excited State 1: 2.095-A 1.9726 eV 628.53 nm f=0.0289 <S**2>=0.847
133A ->135A 0.15036
132B ->133B 0.97172
This state for optimization and/or second-order correction.

Total Energy, E(TD-HF/TD-KS) = -4134.55961738

Copying the excited state density for this state as the 1-particle RhoCI density.

Excited State 2:	2.185-A	2.2930 eV	540.72 nm	f=0.0119	<S**2>=0.944
133A ->134A	-0.39560				
129B ->133B	-0.35588				
130B ->133B	-0.48044				
131B ->133B	0.65271				
Excited State 3:	2.085-A	2.4577 eV	504.46 nm	f=0.0075	<S**2>=0.837
130B ->133B	-0.80478				
131B ->133B	-0.56760				
Excited State 4:	2.114-A	2.5677 eV	482.86 nm	f=0.0002	<S**2>=0.867
133A ->134A	0.29337				
129B ->133B	0.77881				
130B ->133B	-0.25686				
131B ->133B	0.45110				
Excited State 5:	2.131-A	2.6331 eV	470.87 nm	f=0.0079	<S**2>=0.885
133A ->135A	0.15090				
128B ->133B	-0.96252				
Excited State 6:	2.337-A	2.8346 eV	437.39 nm	f=0.0150	<S**2>=1.115
129A ->134A	0.17779				
131A ->134A	0.11818				
133A ->135A	0.51564				
133A ->139A	-0.14941				
127B ->133B	0.72083				
128B ->133B	0.10778				
129B ->134B	0.13897				
131B ->134B	-0.10665				
132B ->133B	-0.10804				

---

6. References

1 R. B. Gaussian 09, M. J. Frisch, G. W. Trucks, H. B. Schlegel, G. E.Scuseria, M. A. Robb, J. R. Cheeseman, G. Scalmani, V. Barone, G. A. Petersson, H. Nakatsuji, X. Li, M. Caricato, A. Marenich, J. Bloino, B. G. Janesko, R. Gomperts, B. Mennucci, H. P. Hratchian, J. V. Ortiz, A. F. Izmaylov, J. L. Sonnenberg, D. Williams-Young, F. Ding, F. Lipparini, F. Egidi, J. Goings, B. Peng, A. Petrone, T. Henderson, D. Ranasinghe, V. G. Zakrzewski, J. Gao, N. Rega, G. Zheng, W. Liang, M. Hada, M. Ehara, K. Toyota, R. Fukuda, J. Hasegawa, M. Ishida, T. Nakajima, Y. Honda, O. Kitao, H. Nakai, T. Vreven, K. Throssell, J. A. Montgomery, Jr., J. E. Peralta, F. Ogliaro, M. Bearpark, J. J. Heyd, E. Brothers, K. N. Kudin, V. N. Staroverov, T. Keith, R. Kobayashi, J. Normand, K. Raghavachari, A. Rendell, J. C. Burant, S. S. Iyengar, J. Tomasi, M. Cossi, J. M. Millam, M. Klene, C. Adamo, R. Cammi, J. W. Ochterski, R. L. Martin, K. Morokuma, O. Farkas, J. B. Foresman, and D. J. Fox, Gaussian, Inc., Wallingford CT, 2016.

2 N. Roques, D. Maspoch, K. Wurst, D. Ruiz-Molina, C. Rovira, J. Veciana, *Chem. Eur. J.*, 2006, **12**, 9238–9253.

3 S. Oda, T. Sugitani, H. Tanaka, K. Tabata, R. Kawasumi, T. Hatakeyama, *Adv. Mater.*, 2022, **34**, 2201778–2201783.
4 T. Lu, F. Chen, *J. Comput. Chem.*, 2012,**33**, 580–592.